

Research article

## A study of organo-modified clay type on pet-clay based nanocomposite properties

Sinem Yelkovan<sup>a</sup>, Demet Yılmaz<sup>a\*</sup>, Kasım Aksoy<sup>b</sup>

<sup>a</sup>Textile Engineering Department, Engineering Faculty, Suleyman Demirel University, Turkey

<sup>b</sup>Biomedical Device Technologies Programme, Technical Sciences Vocational School, Suleyman Demirel University, Turkey

Received 6 January 2013

Revised 21 February 2014

Accepted 24 June 2014

### Abstract

Nowadays, there are many studies regarding with nanocomposite production including nano particles which aimed to gain many properties such as better strength, self-cleaning, and resistance to flammability into synthetic polymers. In nanocomposite production, the materials like clay, silica, metal oxides such as  $\text{TiO}_2$ ,  $\text{Al}_2\text{O}_3$  are used. In present study, three different organically modified montmorillonite (MMT) clays of Cloisite 10A, 15A and 30B (3%) were added into polyethylene terephthalate (PET) polymer. Nanoclay and PET polymer were combined with melt blending method in terms of twin screw extruder. Internal and morphological properties of PET/clay nanocomposites were analyzed with scanning electron microscopy (SEM) images and XRD curves. And also, chemical and thermal properties of nanocomposite samples were studied. The findings and results of nanocomposites were compared with that of PET polymer. At the end of the study, the changes in PET polymer and the effect of clay type on material properties were determined.

©2014 Usak University all rights reserved.

**Keywords:** Nanoclay, polyethylene terephthalate (PET), nanocomposite

### 1. Introduction

Clay is a natural earthy, fine-grained material comprised largely of a group of crystalline minerals known as the clay minerals. Clay minerals are initially characterized by a large active surface area (700-800  $\text{m}^2/\text{g}$  in the case of montmorillonite), a moderate negative surface charge (cation exchange capacity, CEC) and layer morphology. The properties of clays are indeed dominated by their large surface areas compared to the volume of the particle. Among the diverse types of layered silicates, Montmorillonite (MMT) is the most common clay mineral. MMT has been used for nanocomposites production due to its high aspect ratio (size/thickness), and the properties of easily processable and high adsorption ability. MMT particularly plays a part as reinforcement for polymer-clay nanocomposites by virtue of its high platelet aspect ratio, morphology, natural abundance, ecological nature and low cost [1-3].

\*Corresponding author:

E-mail: demetyilmaz@sdu.edu.tr

DOI: 10.12748/ujms.201416498

Nanocomposites are new class of composites that contain relatively small amounts (<10%) of nanometer-sized particles. Typically particles have nano-scale dimensions at least one dimension and they can be mixed in organic polymer matrices. The polymer matrix is the continuous phase and the reinforcement nanoparticles constitute the dispersed phase. The properties and behaviour of the nanoparticles generally control the properties of the composite. In recent years, there has been considerable interest into the usage of nanoparticles to improve the performance properties of the polymer such as mechanical, electrical and barrier properties of polymers. Polymeric nanocomposites get the wide array of property enhancements, e.g., increased stiffness and strength, improved UV resistance, greater dimensional stability, decreased electrical conductivity, and enhanced gas barrier properties [1-4].

The improvements in polymer properties are directly correlated with the dispersion of the particles within the polymeric matrix. There are several techniques used for dispersing particles at a nanoscopic scale, as in situ intercalative polymerization, solution blending and melt intercalation method. The most common method is melt intercalation because the method is eco-friendly, simple and it doesn't require for any solvent [1,3].

From an industrial approach, owing to high costs of development, synthesis and commercialization of new polymers, most researchers look for new materials by reinforcing or blending existing polymers, so the tailor made properties of the materials can be achieved. Therefore, there is great interest in the area of production of polymer nanocomposites. Polymer type for nanocomposite material was first reported as early as 1950. However, it was not widespread until the period of investigation on this type of structures by Toyota researchers. This early work of Toyota group demonstrated the enhanced properties of nylon 6/nanoclay composites [5-8].

In this study, we attempted to fabricate PET-clay nanocomposites through melt-extrusion processing. Many research works have focused on incorporation of nano clay into various polymers however only a few deal with preparation of PET-clay nanocomposites. We set out to investigate the influence of clay type on the surface and internal structure, morphology and thermal properties of the PET-clay composite master batch. In literature, Kim [7], Litchfield *et al.* [8], Scaffaro *et al.* [9], Frounchi *et al.* [10], Barber *et al.* [11], Wang *et al.* [12] and Solis *et al.* [13] studied clay-PET nanocomposite production by melt intercalation method and they worked on the effect of clay amount on nanocomposite properties, particularly clay dispersion in PET polymer matrix and tensile properties. Gashti *et al.* [14] researched the effect of clay type on dyeability of nanocomposites. Calcagno *et al.* [15] determined that clay amount affects the crystallization degree of nanocomposite. Kim [7] also researched oxygen permeability of PET-clay nanocomposites. Scaffaro *et al.* [9] and Ghasemi *et al.* [16] worked on determination of proper clay type. Xiao *et al.* [17], researched the effect of clay on thermal stability of nanocomposites. In the studies, Cloisite 15A and 30B clay types were widely used. However, there are limited findings about Cloisite 10A clay and its comparison with Cloisite 15A and 30B. Therefore, in present study, we focused on the effect of clay type on nanocomposite properties [1,6,8-9,11,19].

## 2. Material and Method

In this study, PET polymer was supplied from SASA Polyester Industries Inc., Turkey. Organically modified montmorillonite clays (Cloisite 10A, 15A and 30B) were used. Montmorillonite is the most widely used layered smectite clay type. It is composed of two silica tetrahedral sheets and a laminae (containing aluminium or magnesium cations)

octahedral sheet. The smectite clay possesses large surface area. In order to utilize their high surface area efficiently, the chemical modification of the clays is necessary. MMT clays are hydrophilic in nature and accessible to intercalation. Na<sup>+</sup> ions are displaced by quaternary-ammonium surfactants and the distance between silicate sheets are expanded. Owing to the organophilic nature, the modified clay is named organophilic clay or organoclay. Alkylammonium ions decrease the surface energy of the clay particles, so that polymers with different polarities can get intercalated between the layers and cause further separation and dispersion of silicate layers [1-3]. In the present study, the fillers, montmorillonite, types of Cloisite 10A, 15A and 30B, were provided from the Southern Clay Products (Table 1). Proper choice of organoclay chemistry is critical and hence we aimed to analyse the different clay types on nanocomposite properties.

**Table 1**

Properties of organoclays [18]

| Characteristics                       | Cloisite 10A       | Cloisite 15A       | Cloisite 30B         |
|---------------------------------------|--------------------|--------------------|----------------------|
| Organic Modifier                      | 2MBHT <sup>a</sup> | 2M2HT <sup>b</sup> | MT2EtOH <sup>c</sup> |
| CEC (meq/100g clay)                   | 125                | 125                | 90                   |
| Moisture (%)                          | <2                 | <2                 | <2                   |
| Weight Loss on Ignition (%)           | 39                 | 43                 | 30                   |
| Density (g/cc)                        | 1.90               | 1.66               | 1.98                 |
| Dry particle size (µm, 50% less than) | 13.67              | 5.88               | 13.68                |

<sup>a</sup> Dimethyl, benzyl, hydrogenated tallow, quaternary ammonium<sup>b</sup> Dimethyl, dehydrogenated tallow, quaternary ammonium<sup>c</sup> Methyl, tallow, bis-2-hydroxyethyl, quaternary ammonium

Prior to melt processing, PET was dried up to 6 hrs at 90°C and nanoclays were waited at 120°C for 1 hr in vacuum oven. There are basically three different processes to make clay-based polymer nanocomposites. As mentioned, melt intercalation method was used for nanocomposite production due to its being eco-friendly and simple method. The content of each clay type in the polymer matrix was ensured to be 3% in weight. Nanocomposites use low filler content (usually <5%) and many studies reported poor miscibility between the organic and inorganic components, leading to agglomeration of the latter, and therefore, weaker materials at higher particle rates [6,19]. Some of the researchers determined the advantages in the mechanical, thermal or optical properties between 1-3% clay usage [3,8,10,12,20]. Therefore, in this study, the clay amount was fixed at 3%.

To provide uniform dispersion of clay pellets in polymer matrix, 30KW PTLE27 twin extruder was used. In extruder, the temperature was arranged at 250°C and the speed of extruder was arranged to 300 rpm. After dried the pellets, in order to examine the clay distribution in polymer matrix, fracture surfaces of specimens were analyzed by SEM. Wide angle XRD of the samples was performed to determine the clay pellets placement in polymer matrix. Thermal properties of nanocomposite were analyzed. The findings were compared with PET polymer.

### 3. Results and Discussion

#### 3.1.SEM Images

In this work, the melt processing of PET nanocomposites based on different types of clay nanoparticles (Cloisite 10A, 15A and 30B) were investigated by SEM. In Fig. 1, it was given surface images of unprocessed PET together with various nanoclay containing PET composites.

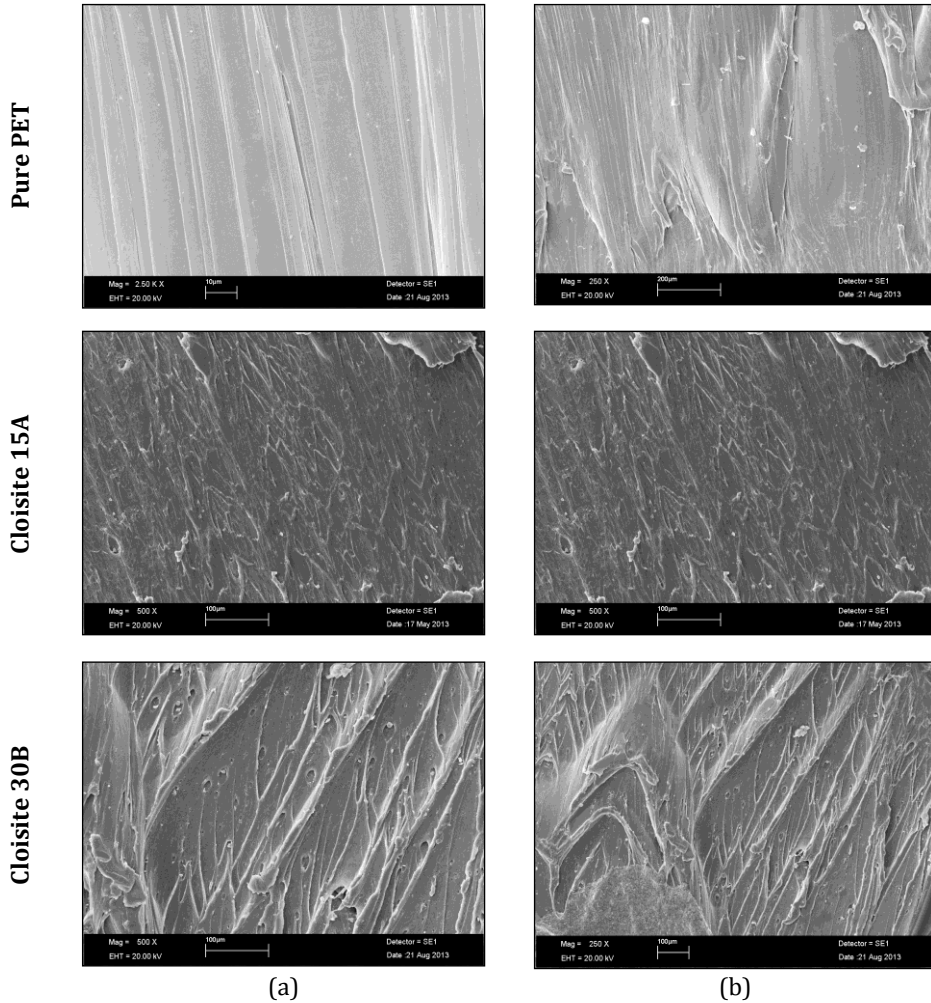


**Fig. 1** Scanning electron micrographs of unprocessed PET, 500X (a) and PET-clay nanocomposites, 250X (b)

As can be seen, unprocessed PET has a relatively smooth and uniform surface. Adding nanoclay particles to the PET matrix leads to changes in the polymer structure. Particle-particle and particle-PET chain interactions result in increased surface roughness. Therefore, there is more torturous appearance in nanocomposites compared to that of pure PET which is in good agreement with Karabulut [6] and Parvinzadeh *et al.* [19]. Crack propagation lines in nanocomposites are long, distant and wider and this may

cause un-uniform images. On the other hand, when the effect of clay types on nanocomposite structures was analyzed, more increased surface roughness was observed in nanocomposite including 30B clay. Crack propagation lines formed with a smaller interlayer distance in 15A comparison with the nanocomposite containing 30B clay type. This leads to more increased surface roughness which was observed with 30B clay particles. This finding was also reported by other authors.

The main difference in clay types is the organic modifier. Natural and unprocessed bentonite clay has been organically modified and surface treatment is based on a quaternary ammonium salts. In commercial area, different organic modifier and salt types have been used and clay is named depending on used modifier type. As seen in Table 1, organic modifier of Cloisite 15A is 2M2HT while Cloisite 30B was modified with a ternary ammonium salt (MT2EtOH) [18]. Modification influences the affinity of the clay particles and between the nanoclay and the matrix. Surface treatments reduce particle-particle attractions. Nanoclay of 15A has methyl groups on its surface and so it is more hydrophobic while nanoclay 30B has more polar groups which makes it more hydrophilic compared to 15A clay. Therefore, 30B has more hydrophilic nano-clay particles. The surface properties of 15A clay make it more compatible with PET molecular chains resulting in only small increases in surface roughness [19]. Another reason may be the particle size. In this work, sizes of clay particles were measured. As seen in Table 1, measured size of 15A particles is smaller than that of the 30B. This may lead to narrower interlayer distance in 15A nanocomposites in comparison to wider crack propagation lines of 30B samples.

### 3.2. Morphological Characterization

The method of X-ray diffraction and scattering is the most widely used techniques for the study of polymer structures. The intensity of the scattered X-rays is measured as a function of scattering direction. The scattering angle, that is, the direction of the scattered beam in relation to the incident beam, is customarily denoted by  $2\theta$  [21].

XRD patterns of Cloisite 10A, 15A and 30B organoclays and of related nanocomposites were shown in Figs. 2-4. The peaks in the graphs,  $2\theta$ , are attributed to the lamellar arrangement of clay platelets. The spacing between clay platelets was determined for the clays and PET/organoclay nanocomposites using the Bragg's law. This distance, corresponding to the  $d_{001}$  plane, is termed the gallery spacing of the clay [22]. In Table 2, d-spacing and  $2\theta$  values of all compositions were given.

Expected properties from polymer based nanocomposite, the main requirement is to obtain uniform dispersion and exfoliated nanocomposite structure. In the case of intercalation, polymer chains are inserted between galleries of the clay, and the d-spacing between the galleries is increased. On the other hand, in the case of exfoliation, these individual silicate layers are distributed randomly in a continuous polymer matrix. The absence of the signal in XRD pattern would be an indication of clay exfoliation. Consequently, characterizing the formation of a nanocomposite requires measurement of the d-spacing by X-ray diffraction analysis.

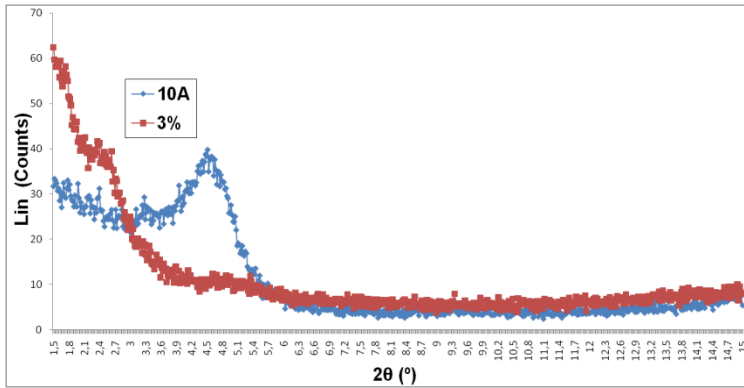


**Fig. 2** X-ray patterns of 10A organoclay and of related nanocomposite materials

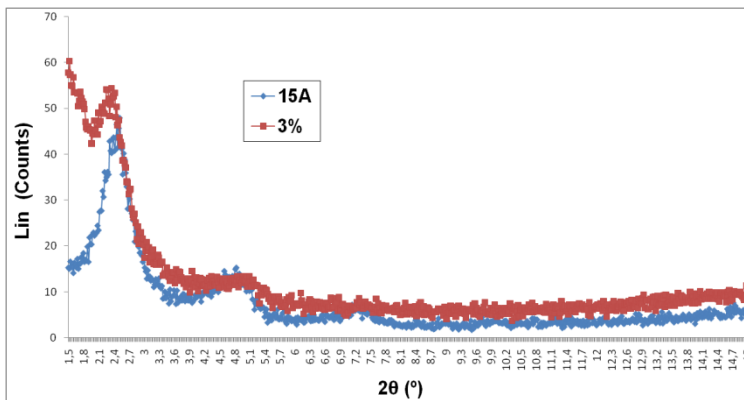


**Fig. 3** X-ray patterns of 15A organoclay and of related nanocomposite materials

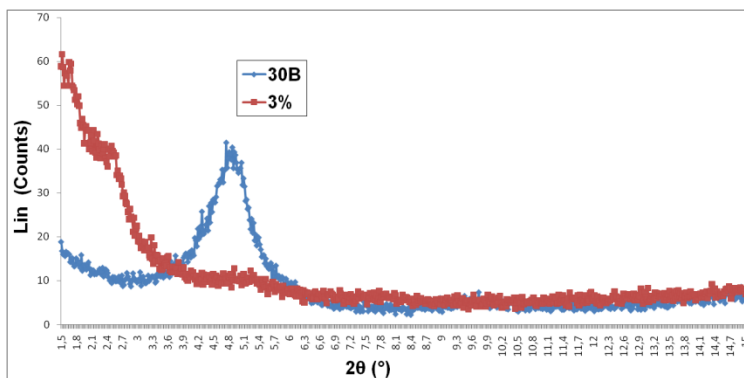


**Fig. 4** X-ray patterns of 30B organoclay and of related nanocomposite materials

When Fig. 2 is analyzed, it was determined that Cloisite 10A has a peak at  $2\theta$  of  $4.3^\circ$ - $4.5^\circ$ , which corresponds to d-spacing of  $20.53$ - $19.62^\circ\text{A}$ . Nanocomposites containing 3% 10A clay displays a peak at about  $2.4^\circ$ , a peak centered at  $36.78^\circ\text{A}$ . d-spacing of  $36.78^\circ\text{A}$  of the nanocomposite produced with 10A clay is relatively higher than that of the Cloisite 10A clay. Interlayer space of the clay in nanocomposite materials increased by  $16.3$ - $17.2^\circ\text{A}$ . This is an indicator of the dispersion of the silicate layers in the polymer matrix. In other

words, the polymer which enters the galleries pushes the platelets far enough apart so that the platelets may not be parallel to each other indicating an effective intercalated structure.

According to Fig. 3, Cloisite 15A organoclay has two distinctive peaks located at  $2.4^{\circ}$ - $2.52^{\circ}$  ( $36.77$ - $35.03^{\circ}\text{A}$ ) and  $4.7^{\circ}$  ( $18.78^{\circ}\text{A}$ ). Nanocomposite master batch containing 15A clay (3wt%) displays similar character and two distinctive peaks were observed at  $2\theta=2.3^{\circ}$  ( $38.38^{\circ}\text{A}$ ) and  $5.0^{\circ}$  ( $17.66^{\circ}\text{A}$ ). There is an increase in d-spacing about  $1.6$ - $3.4^{\circ}\text{A}$ . In comparison to nanocomposites with 10A clay, this generally indicates poor clay delamination because of a large amount of well-defined tactoids. The findings of 10A and 15A clays and their nanocomposites are agreed with Barber *et al.* [11]. On the other hand, the presence of the second order peak suggests that there is still a high degree of layered order present in the clay tactoids.

Cloisite 30A clay type has an apparent peak located at  $2\theta=4.6^{\circ}$ - $4.9^{\circ}$  ( $19.19$ - $18.02^{\circ}\text{A}$ ) while its nanocomposite material showed only an indistinctive shoulder located nearly at  $2\theta=2.2$ - $2.4^{\circ}$  corresponding to a basal interlayer spacing of  $40.12$ - $36.78^{\circ}\text{A}$  (Fig. 4). This increase in the intergallery spacing indicates that effective intercalation process occurred and that the interlayer space of the clay increased by  $18.7$ - $20.7^{\circ}\text{A}$ . However, in nanocomposite material containing 30B clay, there is an indistinctive second peak. Although the gallery spacing of the clay platelets has been increased through the incorporation of PET, there are still clay tactoids.

**Table 2**

XRD data of organoclays and related nanocomposites including 3% clay

| Sample type                 | First peak        |                                  | Second peak       |                                  |
|-----------------------------|-------------------|----------------------------------|-------------------|----------------------------------|
|                             | $2\theta^{\circ}$ | $d_{001}$ ( $^{\circ}\text{A}$ ) | $2\theta^{\circ}$ | $d_{001}$ ( $^{\circ}\text{A}$ ) |
| Cloisite 10A organoclay     | 4.3 - 4.5         | 20.53 - 19.62                    | -                 | -                                |
| Nanocomposite with 10A clay | 2.4               | 36.78                            | 5.0               | 17.66                            |
| Cloisite 15A organoclay     | 2.4 - 2.52        | 36.77 - 35.03                    | 4.7               | 18.78                            |
| Nanocomposite with 15A clay | 2.3               | 38.38                            | 5.0               | 17.66                            |
| Cloisite 30B organoclay     | 4.6 - 4.9         | 19.19 - 18.02                    | -                 | -                                |
| Nanocomposite with 30B clay | 2.2 - 2.4         | 40.12 - 36.78                    | 5.0               | 17.66                            |

XRD results showed that better dispersion of the clay layers was obtained with 30B and then 10A clay types. In these nanocomposite samples, the interlayer spacing of the clay was increased and some extent of exfoliation may occur which should be attributed to diffusion of the PET chains into the clay galleries. However, it is not possible to say that there is a complete exfoliation of the organoclay. On the other hand, the slight increase in the gallery spacing of the Cloisite 15A suggests that very little of the PET intercalated into the gallery space. It seems that interactions between clay particles and polymer chains are not strong enough to disperse hydrophilic nanoclay particles into the PET matrix. In order to verify the morphological changes suggested from the XRD observations made above, transmission electron microscopy (TEM) has been used to directly image the samples.

### 3.3. Chemical Properties

In this study, infrared spectra (FTIR) of clay doped nanocomposite was produced using Cloisite 15A organoclay; unprocessed PET polymer and nanocomposite material containing 3% of Cloisite 15A clay were studied. The spectra of the nanocomposite and ingredients were presented in Fig. 5 and FTIR data were summarized in the Table 3. According to the FTIR analysis, the peak at 3100-2800  $\text{cm}^{-1}$  was the characteristics aromatic and aliphatic C-H stretching peak of PET polymer. This peak appeared at 2957  $\text{cm}^{-1}$  in FTIR spectra of Cloisite 15 nanoclay/PET blend. The peak observed at 1720  $\text{cm}^{-1}$  in the FTIR spectrum of pure PET polymer was characteristic carbonyl peak of ester group and it was emerged at 1713  $\text{cm}^{-1}$  in the IR spectra of Nanoclays/PET.

On the other hand, the peak at 3436  $\text{cm}^{-1}$  was the characteristics primary amine stretching peak and it was observed at 3429  $\text{cm}^{-1}$  in FTIR spectrum of Nanoclay/PET composite. The characteristic C-H stretching peak of Cloisite 15A nanoclay at wavelength of 1047  $\text{cm}^{-1}$  was appeared at the wavelength of 1040  $\text{cm}^{-1}$  in FTIR spectrum of Nanoclay/PET blend. The findings of FTIR analysis proved the presence of PET and Cloisite 15A nanoclay in the structure of Nanoclay/PET composite.

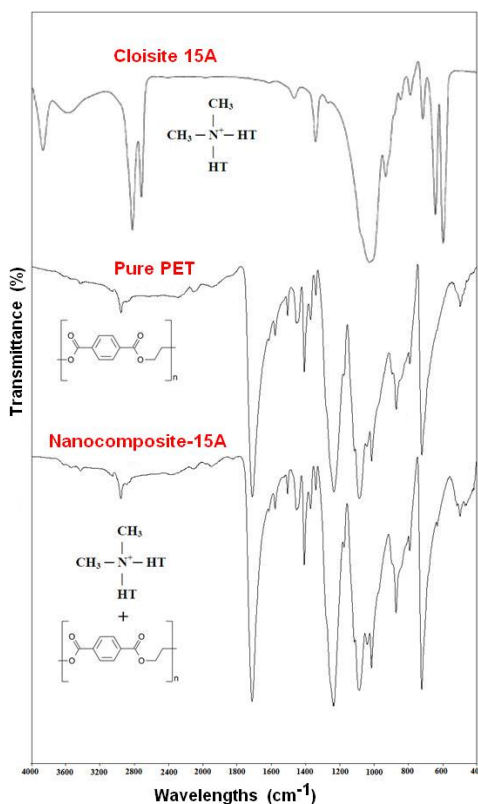


Fig. 5 FTIR spectra of Cloisite 15A, Pure PET polymer and nanocomposite 15A

**Table 3**

Characteristic peaks of Cloisite 15A and pure PET polymer

| Materials                | Peak Frequency<br>cm <sup>-1</sup> | Functional groups                                 |
|--------------------------|------------------------------------|---|
| PET                      | 3100-2800                          | Aromatic and aliphatic C-H stretching peak        |
|                          | 1720                               | Carbonyl peak of ester group                      |
|                          | 1300                               | Stretching peak of ester group                    |
|                          | 1100                               | Bending peak of methylene group                   |
| Cloisite 15A<br>nanoclay | 3436                               | Primary amine (RNH <sub>2</sub> ) stretching peak |
|                          | 2800-2950                          | C-H bending peak in CH <sub>3</sub> alkyl chain   |
|                          | 1047                               | C-H stretching peak                               |

### 3.4. Thermal Properties

Thermal properties of the nanocomposites were investigated by DSC measurements that were carried out on processed PET and on three nanocomposites. In Fig. 6 and Table 4, the calorimetric data for the samples after the first heating were reported. The first heating gives information about the behaviour of the materials.

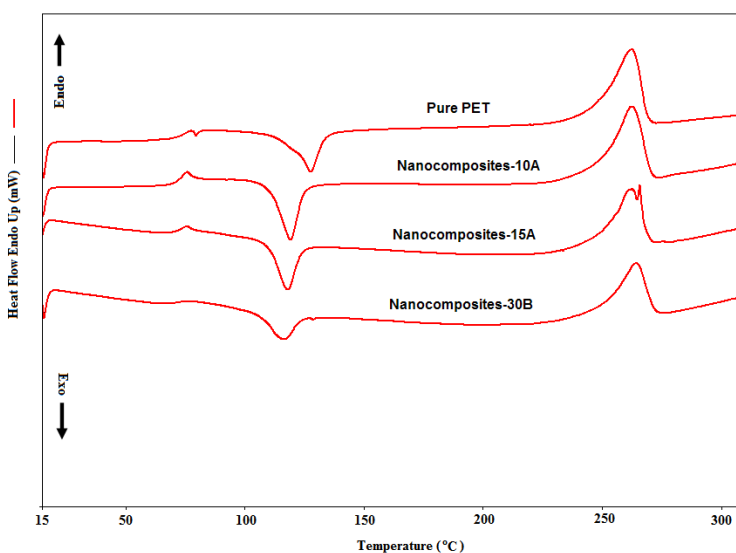


**Fig. 6** DSC curves of unprocessed PET polymer and clay based nanocomposites

When the thermal data are analyzed (Table 4), it was determined that adding clay causes a decrease of the glass transition temperature ( $T_g$ ) and cold crystallization temperature ( $T_c$ ) together with an increase of melting temperature ( $T_m$ ), cold crystallization ( $-\Delta H_c$ ) and melting enthalpy values ( $\Delta H_f$ ). This trend was also observed in literature [9,23-24]. The cold crystallization temperature, melting and cold crystallization enthalpy can be explained with the nucleating effect of the clays. The clay layers can act as a nucleating agent by offering enormous surface area and hence giving rise to higher cold crystallization temperature and enthalpy values, and greater crystallization rate of PET [25]. On the other hand, the decrease of the glass transition and melting temperatures can be interpreted considering a reduction of the molecular weight [9].

**Table 4**

Thermal data collected from DSC thermographs of PET and PET-clay nanocomposite samples

| <b>Melting</b> |                                  |                                   |                                    |                                    |                                   |
|----------------|----------------------------------|-----------------------------------|------------------------------------|------------------------------------|-----------------------------------|
| <b>Sample</b>  | <b>T<sub>g</sub><br/>(°C)</b>    | <b>T<sub>m on</sub><br/>(°C)</b>  | <b>T<sub>m end</sub><br/>(°C)</b>  | <b>T<sub>m peak</sub><br/>(°C)</b> | <b>ΔH<sub>f</sub><br/>(kJ/kg)</b> |
| PET            | 87.83                            | 240.31                            | 260.99                             | 254.54                             | 41.55                             |
| PET/10A        | 77.77                            | 242.59                            | 262.47                             | 254.21                             | 45.19                             |
| PET/15A        | 77.60                            | 255.51                            | 260.25                             | 258.03                             | 40.73                             |
| PET/30B        | 76.26                            | 243.39                            | 263.35                             | 256.36                             | 43.21                             |
| <b>Cooling</b> |                                  |                                   |                                    |                                    |                                   |
| <b>Sample</b>  | <b>T<sub>c on</sub><br/>(°C)</b> | <b>T<sub>c end</sub><br/>(°C)</b> | <b>T<sub>c peak</sub><br/>(°C)</b> | <b>-ΔH<sub>c</sub><br/>(kJ/kg)</b> | <b>X<sub>c</sub><br/>(%)</b>      |
| PET            | 119.28                           | 126.99                            | 126.99                             | 18.59                              | 17.01                             |
| PET/10A        | 110.85                           | 124.44                            | 118.97                             | 21.85                              | 17.29                             |
| PET/15A        | 110.45                           | 123.23                            | 117.62                             | 21.37                              | 14.34                             |
| PET/30B        | 107.02                           | 123.29                            | 115.95                             | 19.65                              | 17.45                             |

The highest reduction in glass transition ( $T_g$ ) and cold crystallization ( $T_c$ ) temperatures were observed of the samples containing 30B clays. On the other hand, samples containing 10A clay, except melting temperature ( $T_m$ ), exhibit the highest temperature and enthalpy values. The most dramatic increase in melting temperature ( $T_m$ ) and the highest reduction in melting enthalpy values ( $\Delta H_f$ ) were occurred in the nanocomposites produced with 15A clay. Similar differences obtained were observed for 15A and 30B clay types by Scaffaro *et al.* [9]. Adding 30B causes higher decrease in glass and cold crystallization temperatures, and leads to an increase lower melting temperature and melting enthalpy values. These changes are definitely more intense when 30B is used.

In the study, initial crystallinity of polymer samples was measured using following formula:

$$X_c = (\Delta H_f - \Delta H_c) \times 100 / \Delta H_f^0 \quad (1)$$

where,  $\Delta H_f$  is the enthalpy of melting,  $\Delta H_c$  is the enthalpy of crystallization,  $\Delta H_f^0$  is the heat of fusion of the completely crystalline materials at the equilibrium melting temperature as 135 kJ/kg [26].

As seen in Table 4, crystallinity values of all samples were in the range of 10-20%. Crystallinity of unprocessed PET and nanocomposites containing 10A and 30B clays are in the same range. However, nanocomposite samples produced with 15A clay type have slightly lower crystallinity value. It was reported that if the crystallinity of a polymer sample is more than 30%, it can alter the mechanical properties noticeably [26]. Therefore, it can be expected that the particles of Cloisite 15A has lower effect on tensile properties of PET polymer. On the other hand, crystallinity values of the nanocomposites containing 10A and 30B clays are slightly higher than that of the PET polymer.

All the results can be explained with degradation of PET matrix occurs when 10A and 30B were used. In particular, on decreasing the molecular weight, the chains become more mobile and more prone to form crystallites. The higher crystalline values observed

for 10A and 30B containing materials are according with their slightly better mechanical performance if compared with the 15A containing ones.

The thermal behaviours of PET and nanocomposite materials were investigated by TGA thermograms. TGA thermograms were presented in Fig. 7. The thermal properties of the samples such as the onset degradation temperature and remaining wt% were summarized in Table 5. All samples exhibited single decomposition step as illustrated in Fig. 7. Nanocomposite samples containing 3% clay particles exhibited less thermal stability than that of unprocessed PET. Clay addition generally causes a decrease in thermal decomposition temperature. On the other hand, decomposition temperature of nanocomposite materials containing 30B clay was found to be the highest while 10A clay type gave the lowest temperature values (Table 5). Lai *et al.* [27] reported that decomposition temperature increases as the particle dispersion improves. This statement confirms higher decomposition temperature values of 10A and 30B clay type. Furthermore, it was seen that the char yield decreased with clay particles. Char residue of the materials produced with 30B clays were slightly higher than 10A and 15A clay type. As stated in literature, char yield increased, flame retardancy was improved [29]. Hence, nanocomposites produced with 30B clay have higher resistance to flame than other clay types.

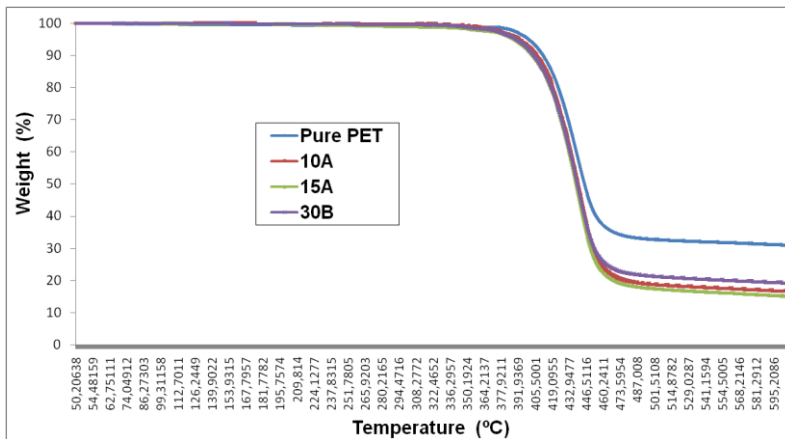


Fig. 7 TGA curves of PET polymer and clay based nanocomposites

Table 5  
Data from TGA Analyses

| Composition                 | T <sub>d</sub> onset (°C) | Remaining wt% |
|-----------------------------|---------------------------|---------------|
| Unprocessed PET             | 313.79                    | 31.93         |
| Nanocomposite with 10A clay | 303.65                    | 16.93         |
| Nanocomposite with 15A clay | 301.42                    | 16.19         |
| Nanocomposite with 30B clay | 307.87                    | 19.68         |

#### 4. Conclusion

In this work, we studied the effect of three different modified montmorillonite clay types (Cloisite 10A, 15A and 30B) on internal and morphological structure and thermal properties of nanocomposite materials. Adding nanoclay in polymer matrix, polymer chains are inserted between galleries of the clay and this causes un-smooth and torturous structure in clay-based nanocomposite samples. Furthermore, d-spacing between the galleries in nanocomposite samples increased. In addition to changes in internal and morphological structure, clay addition to a decrease of the glass transition temperature ( $T_g$ ) and cold crystallization temperature ( $T_c$ ) together with the increase of the melting temperature ( $T_m$ ), cold crystallization ( $-\Delta H_c$ ) and melting enthalpy values ( $\Delta H_f$ ). From interlayer spacing results, better dispersion of the clay layers was determined in the samples containing Cloisite30B and then Cloisite10A clays and these types give higher crystallinity and decomposition temperature values. Therefore, better mechanical performance and flame retardancy may be obtained with 30B and then 10A clays if compared with the 15A containing ones. Finally, clay types and hence the kind of clay modifier have significant effect on nanocomposite properties.

#### Acknowledgement

This work was supported by grants from the Unit of Scientific Research Projects of Isparta in Turkey (Project No: 3516-YL2-13). The authors also wish to express their thanks to SASA Polyester Industries Inc. and Southern Clay companies.

#### References

1. Litchfield DW and Baird DG. The rheology of high aspect ratio nano-particle filled liquids. *Rheology Reviews*, 2006; 1 – 60.
2. Lucilene Betega de Paivaa LB, Moralesa AR and Diaz FRV. Organoclays: properties, preparation and applications. *Applied Clay Science*, 2008; 42: 8 – 24.
3. Pavlidou S and Papaspyrides CD. A review on polymer-layered silicate nanocomposites. *Progress in Polymer Science*, 2008; 33: 1119 – 1198.
4. Şen F, Palancıoğlu H and Aldaş K. Polymeric nanocomposites and their usage areas. *Teknolojik Araştırmalar*, 2010; 7: 111 – 118.
5. Benli B. Nanotechnology with clay based nanostructures since ancient ages. *Kibited*, 2008; 1(6): 143 – 162.
6. Karabulut M. Production and characterization of nanocomposite materials from recycled thermoplastics, Master Thesis, ODTÜ, Science Institute, Ankara, 124, 2003.
7. Kim S. PET Nanocomposites development with nanoscale materials, The University of Toledo, Doctor of Philosophy, 205, 2007.
8. Litchfield D. The manufacture and mechanical properties of PET fibers filled with organically modified montmorillonite, Virginia Polytechnic Institute and State University, PhD thesis, 343, 2008.
9. Scaffaro R, Botta L, Ceraulo M and Mantia F. Effect of kind and content of organo-modified clay on properties of PET nanocomposites. *Journal of Applied Polymer Science*, 2011; 122: 384 – 392.
10. Frounchi M and Dourbash A. Oxygen barrier properties of poly(ethyleneterephthalate) nanocomposite films. *Macromolecule Material Engineering*, 2009; 294: 68–74.

11. Barber G, Calhoun B and Moore R. Poly(ethylene Terephthalate) ionomer based clay nanocomposites produced via melt extrusion. *Polymer*, 2005; 46: 6706-6714.
12. Wang Y, Gao J, Ma Y and Agarwal U. Study on mechanical properties, thermal stability and crystallization behavior of PET/MMT nanocomposites. *Composites*, 2006: 99 – 407.
13. Solis AS, Rejon AG and Manero O. Production of nanocomposites of PET-montmorillonite clay by an extrusion process. *Macromolecular Symp.*, 192, 281 – 292, 2003.
14. Gashti MP and Moradian S. Effect of nanoclay type on dyeability of polyethylene terephthalate/clay nanocomposites. *Journal of Applied Polymer Science*, 2012; 125(5):4109–4120.
15. Calcagno CIW, Mariani CM, Teixeira SR and Mauler RS. Morphology and crystallization behavior of the PP/PET nanocomposites. *Journal of Applied Polymer Science*, 2009; 111: 29 – 36.
16. Ghasemi H, Carreau PJ, Kamal MR and Calderon JU. Preparation and characterization of PET/clay nanocomposites by melt compounding. *Polymer Engineering & Science*, 2011; 51(6): 1178–1187.
17. Xiao W, Yu H, Han K and Yu M. Study on PET fiber modified by nanomaterials: improvement of dimensional thermal stability of PET fiber by forming PET/MMT nanocomposites. *Journal of Applied Polymer Science*, 2005; 96: 2247 – 2252.
18. Southern Clay Products Documents, 2013
19. Parvinezadeh M, Moradian S, Rashidi A and Yazdanshenas M. Surface characterization of polyethylene terephthalate/silica nanocomposites. *Applied Surface Science*, 2009: 2792 – 2802.
20. Yelkovan S and Yilmaz D. Analysis of the effects of nanoclay on PET nanocomposite properties. *Autex Textile Conference*, 22-24 May, Dresden-Germany, 2013.
21. Alyamaç E. Impact modified poly(Ethylene Terephthalate)-organoclay nanocomposites, Master Thesis, ODTÜ, Science Institute, Ankara, 2004.
22. Çalıklı A. Nanokil-polimer kompozitlerin sentez ve karakterizasyonu. <http://acikarsiv.ankara.edu.tr>, 2013-21-01.
23. Bizarria MTM, Giraldo ALFM, Carvalho CM, Velasco JI, Avila MA and Mei LHI. Morphology and thermomechanical properties of recycled PET–organoclay nanocomposites. *Journal of Applied Polymer Science*, 2007; 104: 1839–1844.
24. Todorov LV and Viana JC. Characterization of PET nanocomposites produced by different melt-based production methods. *Journal of Applied Polymer Science*, 2007;106: 1659 – 1669.
25. Ozen İ and Güneş S. Physical and dyeing properties of poly(ethylene terephthalate)/montmorillonite nanocomposite filament yarns. *Polymer Engineering and Science*, 2012.
26. Labde R. Preparation and characterization of polyethylene terephthalate/montmorillonite nanocomposites by in-situ polymerization method, The University of Toledo, Master of Science Degree in Chemical Engineering, 2010.
27. Lai MC, Chang KC, Huang WC, Hsu SC and Yeh JM. Effect of swelling agent on the physical properties of PET–clay nanocomposite materials prepared from melt intercalation approach. *Journal of Physics and Chemistry of Solids*, 2008; 69(5-6): 1371–1374.

28. Arik B, Bozaci E, Demir A and Özdoğan E. Thermogravimetric, microscopic and mechanical analyses of pbt and pet yarns. *Tekstil Ve Konfeksiyon*, 2013; 23(2): 101 – 107.